

# Turbulence structure in thermal convection and shear-free boundary layers

By J. C. R. HUNT†

Department of Applied Mathematics and Theoretical Physics, University of Cambridge,  
Silver Street, Cambridge CB3 9EW

(Received 10 November 1982 and in revised form 20 September 1983)

This paper is a study of turbulence near rigid surfaces, in the absence of any mean shear. Different sources of turbulence are considered, including thermal convection and grid turbulence. It is shown that, if a rigid boundary is introduced into the flow, then for short times the linear theory of Hunt & Graham (1978) reveals the common structure of these flows near the boundary, if the parameters used are the rate of energy dissipation per unit mass  $\epsilon$  and the distance  $z$  from the surface. Over longer times nonlinear effects develop, such as large eddies straining smaller eddies near the boundary. Some new estimates are suggested here and compared with the computations of Biringen & Reynolds (1981) and experiments of Thomas & Hancock (1977).

It is shown that calculations based on the linear theory agree well with many measurements of the vertical profiles of turbulence in thermal convection layers, including those of the vertical variance, the low-frequency end of the spectrum of the vertical turbulence ( $w$ ), the integral scale of  $w$ , and two-point cross-correlations of  $w$ . (The latter was a *prediction*, subsequently tested by atmospheric measurements.) Some discussion of the reasons for this agreement are suggested. The observations of the effects of mean-velocity gradients near the surface are also shown to be consistent with the theoretical arguments proposed here.

---

## 1. Introduction

There are many kinds of turbulence confined between boundaries, where there is no mean flow relative to the boundaries and where the energy for the turbulence is supplied within the fluid.

The examples we shall concentrate on here are: (i) turbulent thermal convection over a rigid surface with no mean velocity past the surface, where the energy is supplied by buoyancy forces acting throughout the interior of the flow (figure 1); and (ii) turbulence produced by grids placed in the flow (figure 2*a*), where either the grids oscillate in a stationary fluid (McDougall 1979) or the flow moves through a grid past a boundary moving at the same speed as the flow (Uzkan & Reynolds 1967; Thomas & Hancock 1977 – hereinafter referred to as TH).

Provided there are no mean velocity gradients near the boundary, turbulence measurements show that these flows are also similar to those where turbulence impinges on density interfaces. One example is the discontinuity in density at liquid–gas interfaces such as occur at the surfaces of stirred vessels or channel flows in chemical processes or at the surfaces of rivers (McDougall 1979; Komori *et al.* 1982; Hunt 1983; Rodi 1980). Another example is where there is a large-enough discontinuity

† Also Department of Engineering, University of Cambridge.

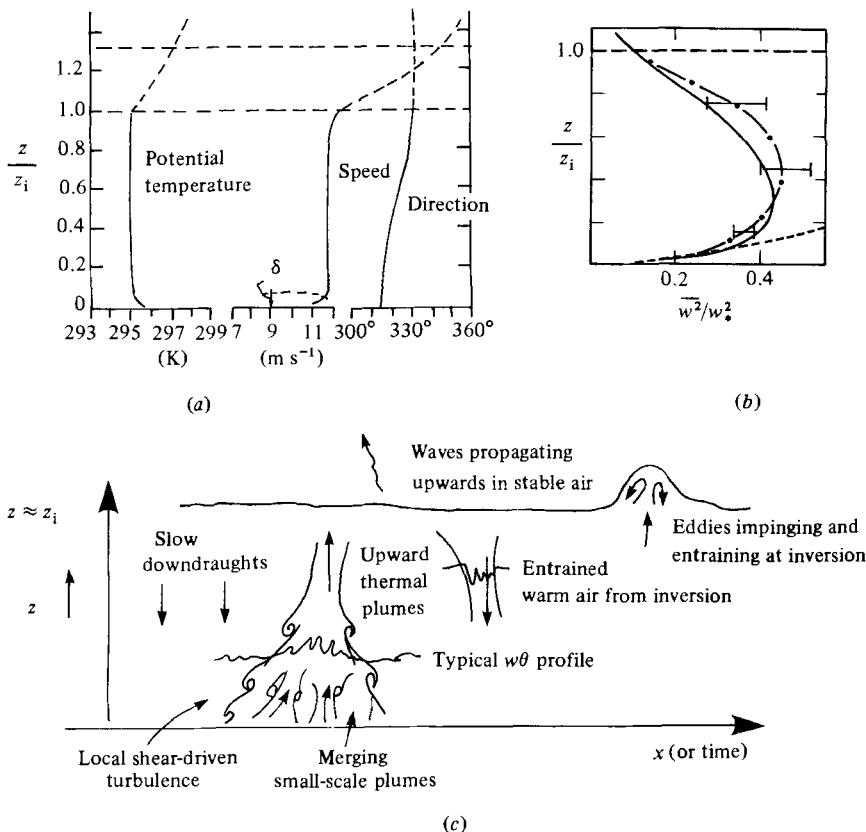


FIGURE 1. Observed features of convective boundary layers. (a) Typical mean profiles (from Kaimal *et al.* 1976). (b) Profiles of vertical turbulence (from Deardorff & Willis 1974) measured from towers (—) and in a laboratory tank (---), and derived from a large-eddy computation (-·-·). (c) Physical mechanisms (Kaimal *et al.* 1976; and others).

in density *gradient* such as may occur at the boundary between a region of thermal convection and stably stratified fluid above or below it (Carruthers & Hunt 1983).

As we shall argue, the essential similarity of these flows is that the average rate of dissipation of turbulent energy per unit mass  $\epsilon$  does not vary appreciably with distance  $z$  from the boundary. The turbulence structure near the boundary is quite different to those where there is a *mean flow* past the boundary, in which case  $\epsilon$  increases rapidly near the surface until it reaches a large limiting value in a small viscous sublayer. More precisely, in these shear flows  $\epsilon \propto z^{-1}$ , as  $z/L \rightarrow 0$ , where  $L$  is a scale of turbulence well away from the boundary.

Shear-free turbulent flows are generally discussed in terms peculiar to their sources of energy. In the case of thermal convection, the turbulence is characterized in terms of the surface heat flux  $Q$ , density  $\rho$ , specific heat  $C_p$ , the surface temperature  $\bar{\theta}_0$ , the depth of the convective layer  $z_i$ , and the distance from the surface, so that by dimensional arguments the mean-square vertical turbulence

and

$$\left. \begin{aligned} \overline{w^2} &\sim \left( \frac{gQz_i}{\rho C_p \bar{\theta}_0} \right)^{\frac{2}{3}} \quad \text{when } z = O(z_i) \\ \overline{w^2} &\sim \left( \frac{gQ}{\rho C_p \bar{\theta}_0} z \right)^{\frac{2}{3}} \quad \text{when } z \ll z_i \end{aligned} \right\} \quad (1.1)$$

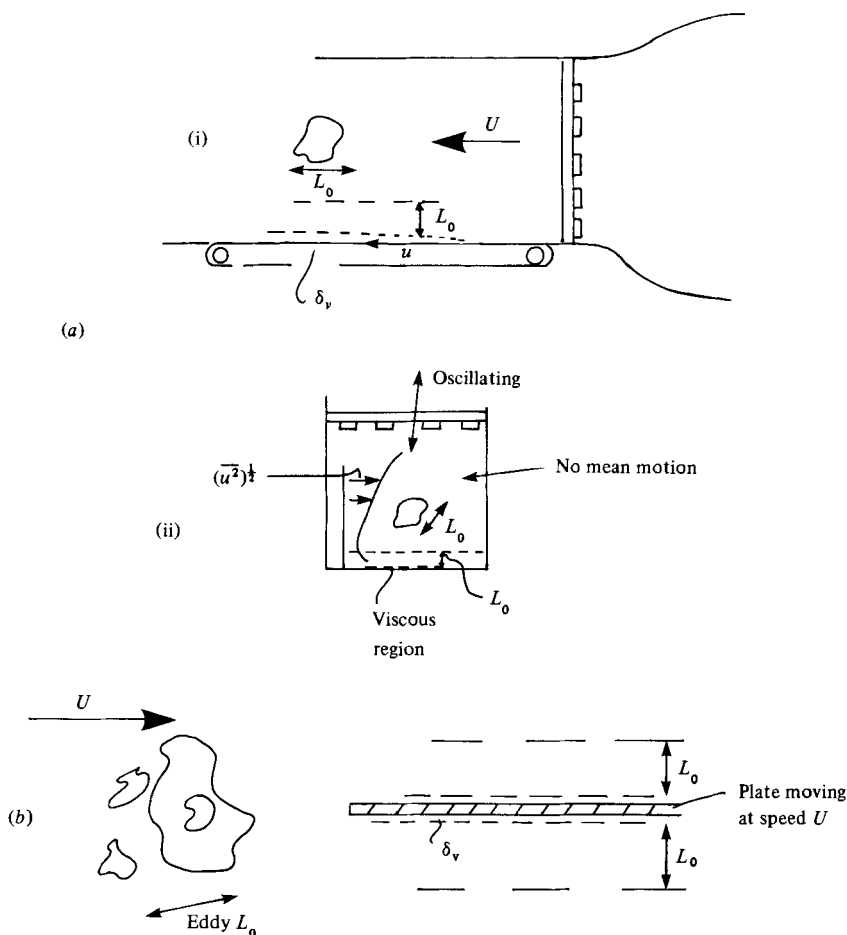


FIGURE 2. Shear-free turbulent boundary layers. (a) (i) Grid turbulence in wind tunnel over a moving wall (Uzkan & Reynolds 1967; Thomas & Hancock 1977). (ii) Grid turbulence in a tank (McDougall 1979). (b) Model problem of Hunt & Graham (1978) (plate moving at a local mean speed  $U$ ).

(Priestley 1959; Kaimal *et al.* 1976). The physical discussion usually given is entirely in terms of the thermal plumes, downdrafts, and entrainment into the plumes. On the other hand, grid turbulence near a moving boundary was analysed by Hunt & Graham (1978; hereinafter referred to as HG) in terms of a characteristic freestream turbulent velocity and lengthscales  $u_0$  and  $L_0$ , and the distance  $z$  from the surface. For example, they and TH found that, near the boundary,

$$\overline{w^2} \sim u_0^2 \left( \frac{z}{L_0} \right)^{3/2}. \quad (1.2)$$

The explanations given there were in terms of eddies impacting on a wall. However, the reader will observe an interesting similarity between (1.1) and (1.2).

The aim of this paper is to show that there are some underlying mathematical and physical similarities and at the same time some important differences in these flows.

The analysis of HG strictly applies to a homogeneous turbulent flow which passes over a semi-infinite rigid surface ( $x > 0$ ), fixed in space but moving at the same velocity  $U$  as the flow (i.e. a moving belt) or over an infinite rigid surface which is introduced into the flow at  $t = 0$ , which also moves at the same speed  $U$  as the flow.

In the linear theory, for times short compared with the ‘turnover’ time of the turbulence, the vorticity is not distorted (except within a thin surface viscous layer). So the effect of the surface is simply to add an *irrotational* flow field to the original turbulence. This idealized linear theory is further developed here in §2.1, with an emphasis on expressing the results in terms of  $\epsilon$ . Recently the effects of the nonlinear processes have been studied by Biringen & Reynolds (1981) using the ‘large-eddy’ approximation to compute this particular turbulent flow. They found that, following the introduction of the boundary, as the turbulence develops, all three components of the turbulence near the boundary are amplified to values greater than predicted by the linear theory. In §2.1.3 a physical explanation and quantitative estimate of this effect is given in terms of the distortion by the large-scale eddies near the boundary of the vorticity of the small-scale eddies, which is a nonlinear process excluded from the linear analysis.

In §2.2 it is argued that the same linear analysis may also be appropriate for the steady state of turbulence near a rigid surface in the absence of shear. Since  $\epsilon$  is approximately constant with height, the mean square vorticity is also approximately constant. To satisfy the latter condition for all scales of motion and the condition at the boundary of zero normal velocity, the simplest form for the turbulent velocity field is that it consists of homogeneous turbulence and an appropriate irrotational velocity field.

Then the results (1.1) and (1.2) follow directly from the theory, and, when expressed in terms of  $\epsilon$ , the constant of proportionality is obtained in terms of the universal Kolmogorov constant for the inertial subrange of turbulence spectra. From the theory other second-order moments and spectra of convective and shear-free turbulence can be calculated. In §3 the theory is compared with previously published measurements of variance and spectra, and also new measurements of two-point cross-correlations in the atmospheric boundary layer (Hunt, Kaimal & Gaynor 1984). In §4 the theory is used to analyse the structure of turbulence in a thin, shear-dominated surface boundary layer when there is deep thermal convection or a deep, shear-free turbulent boundary outside it.

## 2. A theoretical model for the ‘source layer’

### 2.1. Sudden application of a boundary

#### 2.1.1. Defining the model problem

Imagine an approximately homogeneous turbulent velocity field  $\mathbf{u}^{(H)}$  such as might be produced by flow through a grid or produced in the central region between two horizontal planes which are sources and sinks of heat.  $L_0$  is the integral scale and  $u_0$  is the r.m.s. velocity. The large scales of these two kinds of turbulence would be quite different, but the small scales would be similar. Now suppose that at  $t = 0$  a rigid boundary is placed at  $z = 0$ . (If there is a mean velocity  $U$ , the boundary is assumed to move with the flow; figure 2(b).)

On the rigid boundary a thin viscous boundary layer develops with thickness  $\delta_v \sim (t\nu)^{\frac{1}{2}}$  for  $t \ll L_0/u_0$ , within which the velocity components parallel to the surface ( $u, v$ ) decrease to zero (HG). Above this viscous layer there is an inviscid inhomogeneous ‘source’ layer with thickness of order  $L_0$ , which we now analyse.

2.1.2. *Initial development* ( $t \ll L_0/u_0$ )

The idealized problem can be stated as follows:

$$\mathbf{u} = \mathbf{u}^{(H)}(\mathbf{x}, t) \quad (t < 0), \tag{2.1 a}$$

$$\left. \begin{aligned} \nabla \times \mathbf{u} &= \boldsymbol{\omega}^{(H)}(\mathbf{x}, t), \\ \mathbf{u} &= 0 \quad \text{on } z = 0, \quad \mathbf{u} \rightarrow \mathbf{u}^{(H)} \quad \text{as } z \rightarrow \infty. \end{aligned} \right\} \quad (t > 0). \tag{2.1 b}$$

In the limit  $(t\nu)^{1/2}/L_0 \rightarrow 0$ , or  $u_0 L_0/\nu \rightarrow 0$ , the viscous layer is very thin compared with the thickness of the source layer. In the inviscid 'source' layer  $\mathbf{u}$  and  $\boldsymbol{\omega}$  must satisfy

$$\nabla \times \mathbf{u} = \boldsymbol{\omega}, \tag{2.2}$$

$$\frac{\partial \boldsymbol{\omega}}{\partial t} = (-\mathbf{u} \cdot \nabla) \boldsymbol{\omega} + (\boldsymbol{\omega} \cdot \nabla) \mathbf{u} + \nabla p \times \nabla \left( \frac{1}{\rho} \right) \tag{2.3}$$

and

$$\nabla \cdot \mathbf{u} = 0. \tag{2.4}$$

The boundary conditions on  $\boldsymbol{\omega}$  and  $\mathbf{u}$  are

$$\mathbf{u} = \mathbf{u}^{(H)}, \quad \boldsymbol{\omega} = \boldsymbol{\omega}^{(H)} \quad (t < 0), \tag{2.5 a}$$

$$\mathbf{u} \cdot \mathbf{n} = 0 \quad \text{as } \frac{z}{L_0} \rightarrow 0, \quad \mathbf{u} \rightarrow \mathbf{u}^{(H)} \quad \text{as } \frac{z}{L_0} \rightarrow \infty. \tag{2.5 b}$$

In the initial development of the source layer, the terms on the right-hand side of (2.3) for the advection and distortion of the turbulent velocity by the turbulence, and for the generation of vorticity by the buoyancy forces, can be estimated as

$$\frac{\partial \boldsymbol{\omega}}{\partial t} = O\left(\frac{u_0^2}{L_0^2}, \frac{g\bar{\theta}}{\bar{\theta}_0 L_0}\right), \tag{2.6}$$

where  $\bar{\theta}, \theta$  are the mean and fluctuating components of temperature, and  $g$  is the gravitational acceleration.  $\bar{\theta}_0$  is the value of  $\bar{\theta}$  at  $z = 0$ . Taking the values of  $\bar{\theta}^2$  as typical of the central region of a convection zone (scale  $z_1 \sim L_0$ ) from Kaimal *et al.* (1976), we can estimate the value of  $t$  for which the change in  $\boldsymbol{\omega}, \Delta\boldsymbol{\omega}$ , relative to its initial values ( $\sim u_0/L_0$ ) (for energy-containing eddies), is small:

$$\frac{\Delta\boldsymbol{\omega}}{u_0/L_0} \ll 1 \quad \text{if } t \ll \frac{L_0}{u_0} \quad \text{and} \quad t \ll \frac{L_0}{u_0} \left( \frac{L_0 g \bar{w} \bar{\theta}}{\bar{\theta}_0 u_0^3} \right)^{-1}. \tag{2.7 a}$$

In large-scale convection (e.g. in the atmosphere)

$$\frac{\bar{w} \bar{\theta} L_0 g}{u_0^3 \bar{\theta}_0} \sim 1.$$

Thus, if  $t \ll L_0/u_0$ ,  $\Delta\boldsymbol{\omega}$  is negligible and

$$\boldsymbol{\omega} = \boldsymbol{\omega}_H. \tag{2.7 b}$$

Thus initially the vorticity  $\boldsymbol{\omega}$  is not changed; only the boundary condition (2.5 b) is imposed. Therefore the only possible field is the *original* homogeneous velocity  $\mathbf{u}^{(H)}$  plus an irrotational incompressible velocity field. Thus for  $t > 0$

$$\mathbf{u} = \mathbf{u}^{(H)} + \mathbf{u}^{(S)}, \tag{2.8 a}$$

where  $\mathbf{u}^{(S)} = -\nabla\phi$ , and  $\phi$  satisfies

$$\begin{aligned} \nabla^2\phi = 0 \quad \text{subject to} \quad \frac{\partial\phi}{\partial z} = \mathbf{u}^{(H)} \cdot \mathbf{n} \quad \text{as} \quad \frac{z}{L_0} \rightarrow 0, \\ \nabla\phi \rightarrow 0 \quad \text{as} \quad \frac{z}{L_0} \rightarrow \infty. \end{aligned} \quad (2.8b)$$

We now summarize the results for spectra, variances and correlations derived in HG, but expressing them in more general terms for wider application. Note that the one-dimensional spectra are 'two-sided' in the sense that integrals are taken from  $-\infty$  to  $+\infty$ , e.g.

$$\overline{w^2} = \int_{-\infty}^{\infty} \Theta_{33} d\kappa_1,$$

but in the following discussion we only refer to positive values of  $\kappa_1$ .

(i) *Near the surface.* At the surface the vertical velocity is zero and the energy of the horizontal components is equal to the energy in all three components of  $\mathbf{u}^{(H)}$  as both  $z/L_0 \rightarrow 0$  and  $z\kappa_1 \rightarrow 0$ :

$$\Theta_{33}(\kappa_1) \rightarrow 0, \quad \Theta_{11} + \Theta_{22} = \sum_{i=1}^3 \Theta_{ii}^{(H)}(\kappa_1). \quad (2.9a)$$

For very small scales of spectra, if  $z\kappa_1 \rightarrow \infty$

$$\Theta_{ij}(\kappa_1) \rightarrow \Theta_{ij}^{(H)}(\kappa_1). \quad (2.9b)$$

Thus

$$\overline{w^2} \rightarrow 0, \quad \overline{u^2} + \overline{v^2} = \overline{q^2}^{(H)} \quad \text{as} \quad \frac{z}{L_0} \rightarrow 0, \quad (2.10a)$$

where  $\overline{q^2} = \overline{u^2} + \overline{v^2} + \overline{w^2}$ . Note that, although  $\overline{q^2} = \overline{q^2}^{(H)}$  as  $z/L_0 \rightarrow 0$  and for  $z/L_0 \rightarrow \infty$ , this equality does not hold for *all*  $z/L_0$ . If  $\mathbf{u}^{(H)}$  is isotropic then

$$\overline{u^2} = \overline{v^2} = 1.5\overline{u^2}^{(H)} \quad \text{as} \quad \frac{z}{L_0} \rightarrow 0. \quad (2.10b)$$

(ii) *Spectra.* The theoretical forms of the spectra are shown in figure 3. The low-frequency spectra of  $u$  and  $v$  near the surface are such that  $\Theta_{11}(\kappa_1 \rightarrow 0)$  is not changed, whereas  $\Theta_{22}(\kappa_1 \rightarrow 0)$  is increased by as much as  $\Theta_{33}(\kappa_1 \rightarrow 0)$  is reduced, i.e.

$$\Theta_{11}(\kappa_1 \rightarrow 0, z) = \Theta_{11}^{(H)}(\kappa_1 \rightarrow 0) \quad \text{or} \quad \overline{u^2} L_x^{(u)} = \overline{u^2}^{(H)} L_x^{(u, H)}, \quad (2.11a)$$

while

$$\Theta_{22}(\kappa_1 \rightarrow 0, z \rightarrow 0) = \Theta_{22}^{(H)}(\kappa_1 \rightarrow 0) + \Theta_{33}^{(H)}(\kappa_1 \rightarrow 0), \quad (2.11b)$$

where  $L_x^{(u)}$  is the integral scale of  $u$  in the  $x$ -direction. The changes in  $\Theta_{11}(\kappa_1)$  occur where  $\kappa_1 \sim 1/z$ . An important consequence of these results is that the spectra of  $u$  and  $v$  near the boundary depend on the form of the spectra of  $u$ ,  $v$  and  $w$  in the homogeneous region.

The one-dimensional spectrum  $\Theta_{33}(\kappa_1)$  of  $w$ , the component normal to the boundary, is given by (2.55) of HG, which can be re-expressed in terms of the energy-spectrum tensor  $\Phi_{33}$  of the homogeneous turbulence, viz

$$\Theta_{33}(\kappa_1) = \int_{-\infty}^{\infty} \int_{-\infty}^{\infty} (1 - 2 \cos \kappa_3 z e^{-k_{12} z} + e^{-2k_{12} z}) \Phi_{33}^{(H)} d\kappa_2 d\kappa_3, \quad (2.12a)$$

where  $k_{12} = (\kappa_1^2 + \kappa_3^2)^{1/2}$ , and, if the homogeneous turbulence is isotropic,

$$\Phi_{33}^{(H)} = \frac{E^{(H)}(k) k_{12}^2}{4\pi k^4}, \quad (2.12b)$$

where  $k^2 = \kappa_1^2 + \kappa_2^2 + \kappa_3^2$  and  $E^{(H)}(k)$  is the energy spectrum (see Batchelor 1953, chap. 3). Inspection of (2.12) and the asymptotic analysis of HG show that, as

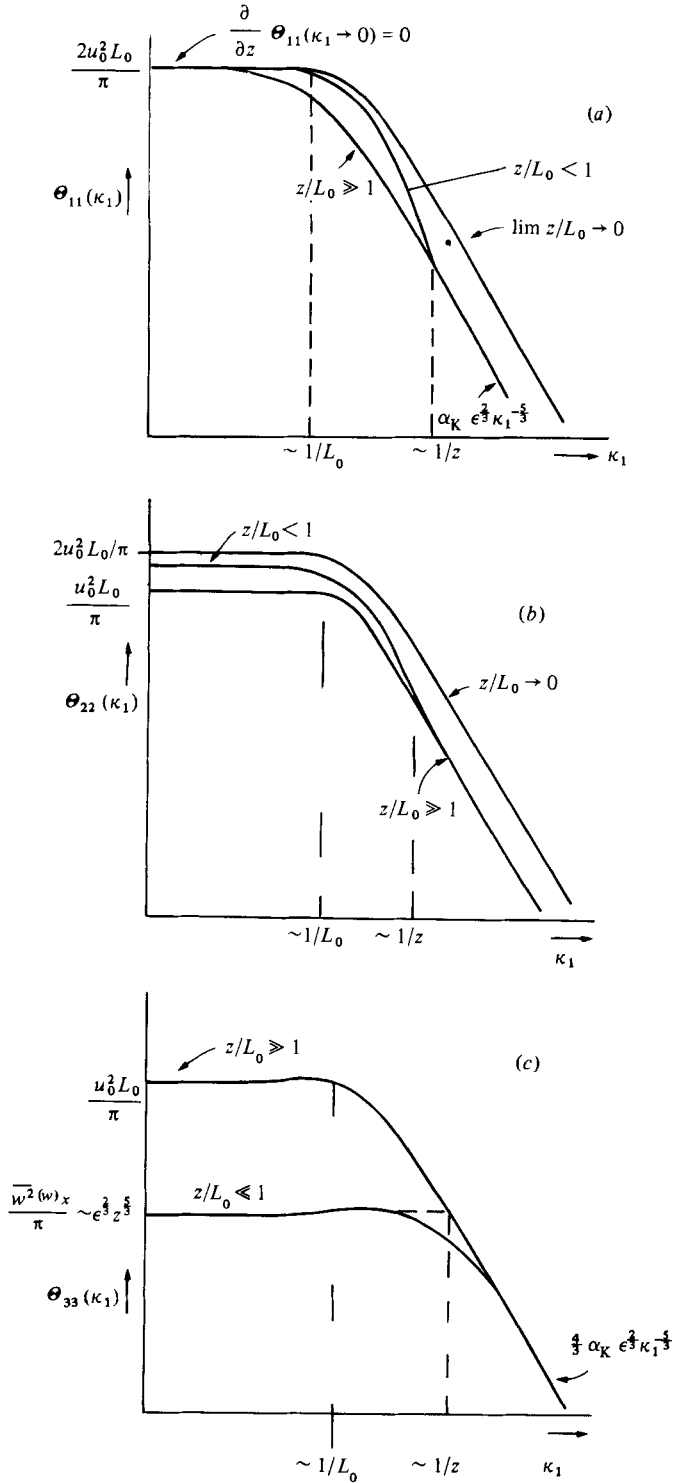


FIGURE 3. Schematic diagrams of the one-dimensional spectra in shear-free boundary layers of the different velocity component: (a)  $u$  or  $x$ -component; (b)  $v$  or  $y$ -component; (c)  $w$  or  $z$ -component. Note that  $L_0$  is the integral scale or the  $w$ -component in the homogeneous isotropic turbulence outside the shear-free boundary layer.

$z/L_0 \rightarrow 0$ , only the high wavenumbers ( $kL \gg 1$ ) contribute to the integral, and therefore only the high-wavenumber form of  $E(k)$  is significant. But, at high wavenumbers ( $kL_0 \gg 1$ ),  $E(k)$  has the universal Kolmogorov form

$$E(k) = \frac{55}{9} \alpha_K \epsilon^{\frac{2}{3}} k^{-\frac{5}{3}}. \quad (2.12c)$$

The constant  $\alpha_K$  is chosen so that at high wavenumbers the homogeneous one-dimensional spectrum has the form

$$\Theta_{11}^{(H)}(\kappa_1) = \alpha_K \epsilon^{\frac{2}{3}} \kappa_1^{-\frac{5}{3}}. \quad (2.12d)$$

The results of many measurements indicate that  $\alpha_K = 0.25 \pm 0.05$  (Townsend 1976, p. 98). Thus, by combining (2.1a-c) it follows that, as  $z/L_0 \rightarrow 0$ ,  $\Theta_{33}(\kappa_1)$  depends only on  $z$ ,  $\alpha_K$ , and  $\epsilon$ ; in other words, the spectrum of  $w$  only depends on eddies in the homogeneous turbulence that are small compared with  $z$  and are not 'blocked' by the boundary. These eddies are independent of the low-wavenumber part of the spectrum of  $\mathbf{u}^{(H)}$ .

Asymptotic analysis of the resulting integral, confirmed by numerical computation, shows that, as  $z/L_0 \rightarrow 0$ ,

$$\Theta_{33}(\kappa_1 \rightarrow 0) = \frac{\overline{w^2} L_x^{(w)}}{\pi} = \gamma_\Theta \alpha_K \epsilon^{\frac{2}{3}} z^{\frac{5}{3}}, \quad (2.13a)$$

where†

$$\begin{aligned} \gamma_\Theta &= \frac{2\Gamma(\frac{1}{3})}{\Gamma(\frac{5}{6})} \left[ \frac{9}{5} \frac{2^{\frac{2}{3}}}{\pi^{\frac{1}{2}}} \Gamma(\frac{7}{3}) - \frac{9}{\Gamma(\frac{1}{6})} \right] \\ &= 4.50. \end{aligned} \quad (2.13b)$$

In figure 8 a comparison is made between this limiting form and the value of  $\Theta_{33}$  when  $\kappa_1 \ll L_0^{-1}$  and  $z/L_0$  is small but finite. For the latter computation it is necessary to know the form of  $E(k)$  over the whole wavenumber range. So  $E(k)$  is taken to have the commonly observed form

$$E^{(H)}(k) = \left(\frac{55}{9} \alpha_K\right) \frac{\epsilon^{\frac{2}{3}} k^4}{(g_2 L_0^{-2} + k^2)^{\frac{7}{2}}}, \quad (2.13c)$$

where  $g_2 = 0.56$ , as in the von Kármán spectrum, defined by HG in their equations (2.62) and (2.63).

(iii) *Variances.* Computations of  $\overline{u^2}$ ,  $\overline{w^2}$  as functions of  $z/L_0$  (see figure 4) show that, if the initial turbulence is isotropic, the horizontal variances  $\overline{u^2}/\overline{u^{2(H)}}$ ,  $\overline{v^2}/\overline{v^{2(H)}}$  are equal and increase above their homogeneous value within a distance of about  $0.6L_x^{(w, H)}$ , or  $0.3L_x^{(u, H)}$  of the surface.  $w^2$  decreases to zero monotonically over a distance of about  $2L_x^{(w, H)}$  or  $L_x^{(u, H)}$ . The kinetic energy does not change monotonically; in fact  $q^2/q^{2(H)}$  decreases to just less than 1.0 when  $0 < z < 2L_x^{(w, H)}$ , its minimum value being 0.85.

By integrating (2.12a) and using (2.12b, c),  $\overline{w^2}$  can be expressed in the local variables  $\epsilon$  and  $z$  when  $z/L_0 \ll 1$  as

$$\overline{w^2} = \gamma_w \alpha_K \epsilon^{\frac{2}{3}} z^{\frac{5}{3}}, \quad \text{where } \gamma_w = 7.16, \quad (2.14a)$$

$$\approx 1.8\epsilon^{\frac{2}{3}} z^{\frac{5}{3}} \quad \text{if } \alpha_K = 0.25. \quad (2.14b)$$

From (2.13) and (2.14) the integral scale for  $L_x^{(w)}(z)$  is given by

$$L_x^{(w)}\left(\frac{z}{L_0} \rightarrow 0\right) = \frac{4\pi z}{7.2} = 1.96z. \quad (2.15)$$

† The factor  $\frac{9}{10}$  was mistakenly 1.0 in HG, which explains why  $\gamma_\Theta$  is 4.5 rather than 4.0 in HG. The computed spectra in HG are correct. This error was pointed out by Mr H. Wong.

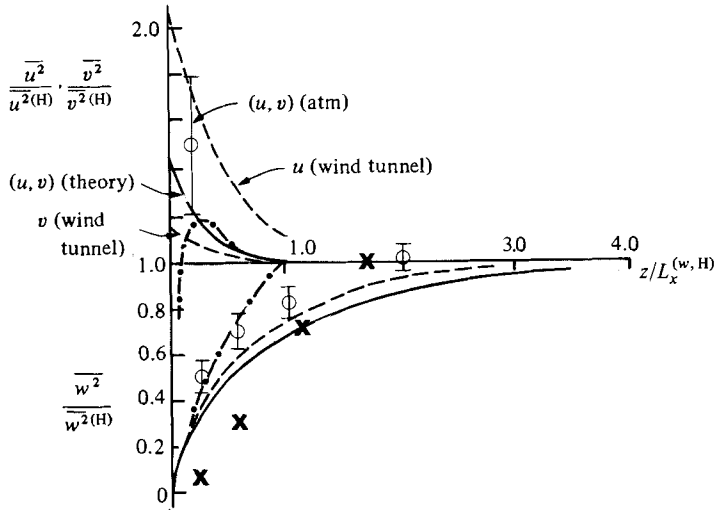


FIGURE 4. Variation of  $\overline{u^2}, \overline{v^2}, \overline{w^2}$  near  $z = 0$  for convective and shear-free boundary layers:  $\Phi$ , CBL – as summarized by Caughey & Palmer (1979);  $\times$ , mixing-box turbulence near rigid lid (McDougall 1979); ---, wind-tunnel moving floor (Thomas & Hancock 1977); —, theory (Hunt & Graham 1978); -·-·-, laboratory convection (Adrian & Ferreira 1979). Superscript (H) refers to the values in the homogeneous turbulence outside the boundary layers, or in the centre of a convective layer.

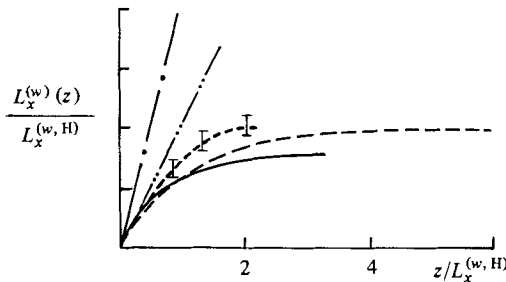


FIGURE 5. Integral scale of the vertical component of turbulence:  $\cdot\cdot\cdot\cdot\cdot$ , CBL measurements;  $\cdot\cdot\cdot\cdot\cdot$ , measured asymptote  $L_x^{(w)} = z$  (Caughey & Palmer 1979); ---, SFBL measurements (Thomas & Hancock 1977); —, theory (Hunt & Graham 1978); -·-·-, theoretical asymptote  $L_x^{(w)} = 2z$ .

The latter limit is in fact only reached to within 20% when  $z/L_x^{(w,H)} < 0.01$ . See figure 5, in which the vertical profile of  $L_x^{(w)}$  is plotted for the energy spectrum of (2.13c).

(iv) *Making rough estimates.* A straight-line graphical construction (following Kaimal 1973) on the graph of  $\Theta_{33}$  gives rough estimates which may be adequate for some practical purposes: for  $z/L_0 \ll 1$

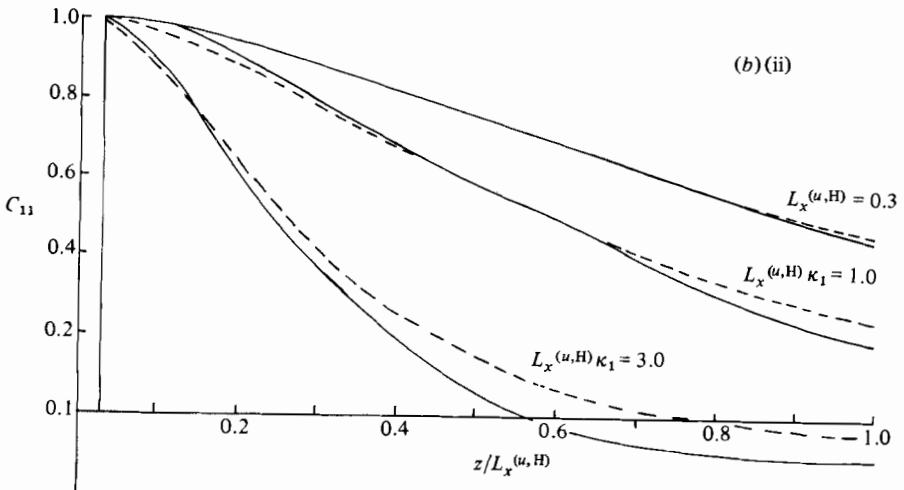
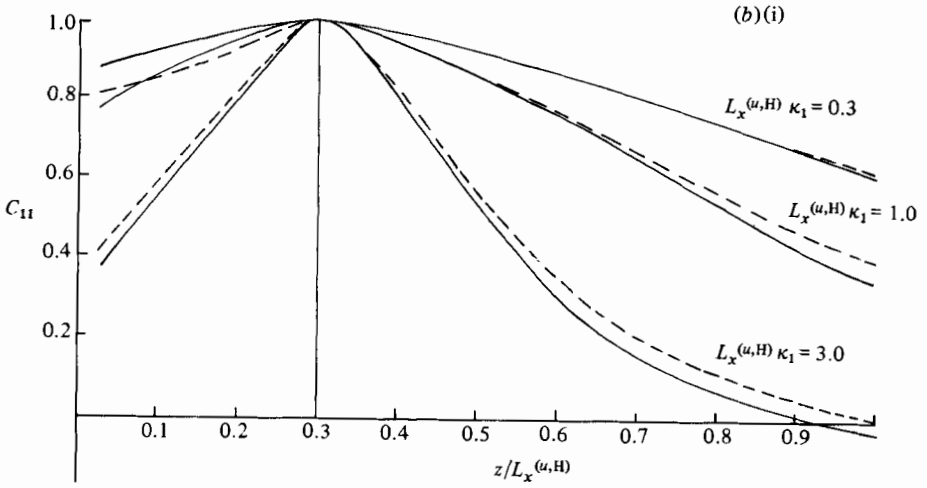
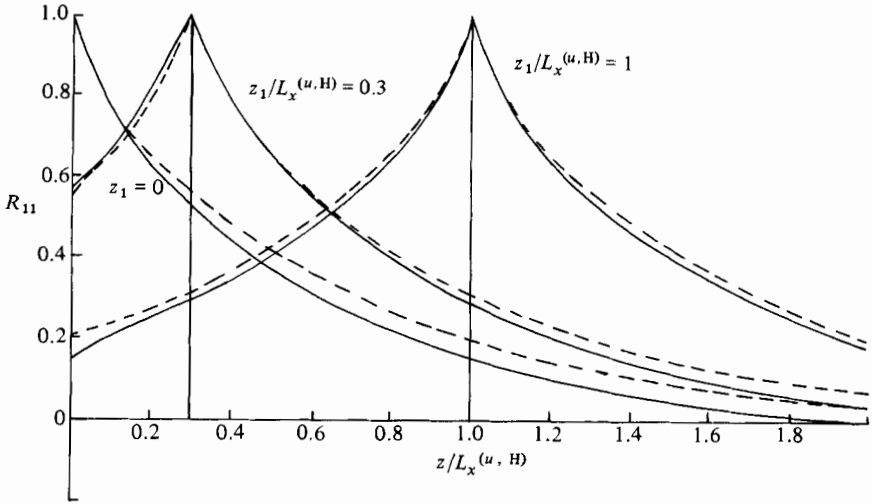
$$\begin{aligned} \Theta_{33} &\approx \frac{4}{3}\alpha_K \epsilon^{\frac{2}{3}} z^{\frac{5}{3}} \left( \kappa_1 < \frac{1}{z} \right), \\ &\approx \frac{4}{3}\alpha_K \epsilon^{\frac{2}{3}} \kappa_1^{-\frac{5}{3}} \left( \kappa_1 > \frac{1}{z} \right). \end{aligned} \tag{2.16}$$

Then, by integration of (2.16),

$$\overline{w^2} = 6.7\alpha_K \epsilon^{\frac{2}{3}} z^{\frac{5}{3}},$$

which gives  $\overline{w^2}$  close to the exact value in (2.14a). But the estimate for  $\Theta_{33}(\kappa_1 \rightarrow 0)$  is a factor of 3 too small.

(v) *Cross-correlations and coherences.* A revealing way of studying the effect of a



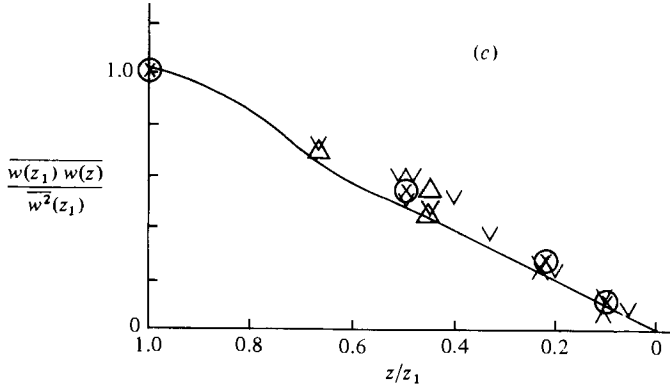


FIGURE 6. Cross-correlations between turbulent velocities at different heights in a SFBL. (a) Theoretical curves for  $R_{11}(z_1, z_2)$  for  $z_1 = 0, 0.3L_x^{(u, H)}, 1.0L_x^{(u, H)}$ . (b) Cospectra of  $u_i$  at  $z_1$  and  $z_2$  at three wavenumbers, computed with the cospectra in homogeneous turbulence: (i)  $z_1 = 0.3L_x^{(u, H)}$ ; (ii)  $z_1 = 0$ . (c) Cross-correlation of vertical velocity  $w(z_1)w(z)/w^2(z_1)$ , normalized on the variance at  $z_1$ , theory (—) and atmospheric measurements. Measurements at Boulder Atmospheric Observatory (Hunt *et al.* 1984):

	Dates	Ratio of the height $z_1$ of the higher point to the inversion height $z_1$ /Monin-Obukhov length	
		$= z_1/z_i$	$= z_i/L_{MO}$
x	28.4.78	0.21	7
⊙	25.4.78	0.084	350
^	26.4.78	0.21	30
v	22.9.78	0.17	≈ 100
△	22.9.78	0.10	≈ 100

boundary on a turbulent flow is to calculate and measure cross-correlations  $R_{ii}$  and coherences  $C_{ii}$  of the  $i$ th components of velocity at two heights  $z_1$  and  $z$ , where

$$R_{ii} = \frac{\overline{u_i(z_1) u_i(z)}}{[\overline{u_i^2(z_1)} \overline{u_i^2(z)}]^{1/2}} \tag{2.17a}$$

and

$$C_{ii} = \frac{\Theta_{ii}(z_1, z; \kappa_1)}{[\Theta_{ii}(z_1, \kappa_1) \Theta_{ii}(z, \kappa_1)]^{1/2}} \quad (\text{no summation}) \tag{2.17b}$$

These functions are also used to calculate fluctuating wind loads on structures and to calculate the dispersion of clouds of contaminant.  $R_{11}$  and  $C_{11}$  have been computed for various values of  $z_1, z_2$  and  $\kappa_1$  from equations (2.48) and (2.50) in HG, using the form of  $E(k)$  given previously in (2.13c). The results for  $R_{11}$  and  $C_{11}$  plotted in figures 6(a, b) show that the boundary has rather little effect as might be expected from the fact that the form of the spectrum of  $\Theta_{11}$  in figure 3 does not change appreciably near the boundary.

However, figure 6(c) shows that the effects of the boundary on  $R_{33}$  and  $C_{33}$  are large, which can be understood better by considering the limiting form for  $R_{33}$  near the boundary. For arbitrary  $z_1$  and  $z$

$$\overline{w(z_1) w(z)} = \iiint_{-\infty}^{\infty} [\cos(\kappa_3(z_1 - z)) - e^{-\kappa_{12} z} \cos \kappa_3 z_1 - e^{-\kappa_{12} z_1} \cos \kappa_3 z + e^{-\kappa_{12}(z_1 + z)}] \frac{k_{12}^2 E(k)}{4\pi k^4} d\kappa_1 d\kappa_2 d\kappa_3. \tag{2.18a}$$

In the limit that  $z_1 \ll L_0$ , only the universal high-wavenumber form of  $E(k)$  is relevant. Close to  $z_1$ , where  $|z_1 - z| \ll z_1 \ll L_0$ , by normalizing the integral in terms of  $z_1$ , (2.18a) reduces to

$$\overline{w(z_1)w(z)} = \overline{w^2}(z_1) - \frac{55}{9}\alpha_K \epsilon^{\frac{2}{3}} \frac{z_1 - z}{z_1^{\frac{4}{3}}} \int_0^\infty \int_0^\infty f(\bar{\kappa}_3, \bar{k}_{12}) e^{-\bar{k}_{12}} d\bar{k}_{12} d\bar{\kappa}_3,$$

where

$$f(\ ) = \frac{\bar{k}_{12}^3 (\bar{\kappa}_3 \sin \bar{\kappa}_3 + \bar{k}_{12} \cos \bar{\kappa}_3 - \bar{k}_{12} e^{-\bar{k}_{12}})}{(k_{12}^2 + \bar{\kappa}_3^2)^{\frac{17}{2}}}. \quad (2.18b)$$

Expressing the integrand in terms of polar coordinates, and integrating first with respect to the radial coordinate, the integral can be derived in terms of gamma function. Then, using (2.14),

$$\overline{w(z_1)w(z)} = \overline{w^2}(z_1) \left( 1 - \frac{0.33(z_1 - z)}{z_1} \right) \quad (2.18c)$$

or

$$R_{33} = \left( 1 - \frac{0.6(z_1 - z)}{z_1} \right). \quad (2.18d)$$

By comparison, in homogeneous turbulence when  $|z_1 - z| \ll L_0$ ,

$$R_{33}^{(H)} = 1 - O\left[\left(\frac{|z_1 - z|}{L_0}\right)^{\frac{2}{3}}\right] \quad (2.18e)$$

Close to the boundary where  $z \ll z_1 \ll L_0$ , (2.18a) reduces to

$$\overline{w(z_1)w(z)} = \frac{55}{9}\alpha_K \epsilon^{\frac{2}{3}} \frac{z}{z_1^{\frac{4}{3}}} \int_0^\infty \int_0^\infty f d\bar{k}_{12} d\bar{\kappa}_3 \quad (2.19a)$$

$$= \overline{w^2}(z_1) \times 1.02 \frac{z}{z_1} \quad (2.19b)$$

and  $R_{33} = 1.02(z/z_1)^{\frac{2}{3}}$ . Inspection of the computed form in figure 6(c) shows that to a good approximation near the boundary of these turbulent layers the cross-correlation is given by

$$\frac{\overline{w(z_1)w(z)}}{\overline{w^2}(z_1)} \approx \frac{z}{z_1}. \quad (2.19c)$$

Comparing (2.18d) and (2.18e) and looking at fig. 6c show how the cross-correlation of the vertical velocity at two points a given distance  $|z_1 - z|$  apart is very much less near the boundary than in the homogeneous turbulence far from the boundary. This is because near the boundary the vertical velocity of the large-scale eddies is blocked by the boundary. So  $\overline{w(z_1)w(z)}$  is partly determined by these blocked eddies of scale  $z_1$  and partly weakly correlated small eddies with scale  $O(z)$ . The latter make much less contribution.

### 2.1.3. Developing state

The equation (2.6) for the development of the vorticity in the source layer shows that there must be some distortion of the initial vorticity  $\omega^{(H)}$  both by the turbulence itself and, if they are present, by buoyancy effects.

We shall find it useful to develop a physical model which gives an order-of-magnitude estimate for the change in the turbulence by nonlinear vorticity-distortion processes near the boundary. (We shall discuss the nonlinear buoyancy effects in §2.2). Essentially we estimate distortions of small-scale turbulent vorticity (on a scale much less than  $z$ ) by larger eddies which are of the order of  $z$ , following the discussion by

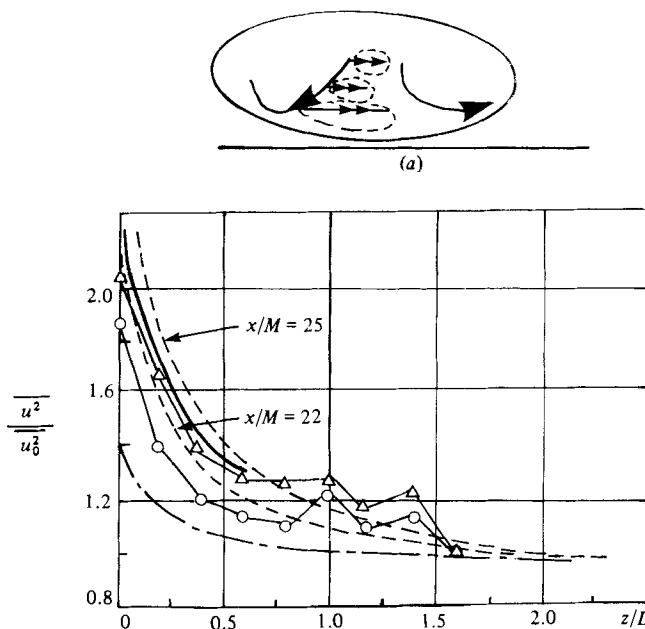


FIGURE 7. (a) Vorticity vector of a small eddy ( $\rightarrow\rightarrow$ ) being stretched by the streamlines ( $\rightarrow$ ) of a large eddy impinging onto the surface. (b) Variations of  $u_1$  variances: measurements by Thomas & Hancock (1977) (---), Biringen & Reynolds' (1981) computations at  $T = 100$  ( $\circ$ ) and  $T = 360$  ( $\triangle$ ); linear theory of Hunt & Graham (1978) (-----); estimate of nonlinear correction  $1 + \frac{1}{3}(L_0/z)^{\frac{1}{2}}$  (—).

Townsend (1976, pp. 99, 100). The components of vorticity  $\omega_x, \omega_y$  of eddies on this scale are systematically *stretched* by larger eddies as they impinge on the boundary by  $O[(L_0/z)^{\frac{1}{2}}]$ . Upward movements have less effect. Consequently, by analogy with the amplification of small-scale turbulence in the straining motion at the front stagnation point of a sphere (Durbin 1981), the small-scale horizontal turbulence  $\overline{u^2}, \overline{v^2}$  in the source layer is amplified by this mechanism by  $O[(L_0/z)^{\frac{1}{2}}]$  (figure 7a). The eddies that are large compared with  $z$  approach the surface too slowly to have much effect on a timescale  $z/u_0$ . Thus in the surface layer the rate of increase of  $\overline{u^2}$  and  $\overline{v^2}$  is estimated to be

$$\frac{1}{\overline{u^2}} \frac{d\overline{u^2}}{dt} \sim \frac{1}{\overline{v^2}} \frac{d\overline{v^2}}{dt} \sim \frac{u_0}{L_0}, \quad (2.20a)$$

and when

$$t \sim T_L \sim L_0/u_0$$

$$\overline{u^2} \approx \overline{u^2} \left( 1 + \frac{1}{3} \left( \frac{L_0}{z} \right)^{\frac{1}{2}} \right). \quad (2.20b)$$

The amplification of  $\overline{w^2}$  is not large, because of the blocking by the surface. (The factor in (2.20b) is chosen to agree with Durbin's (1981) calculation for isotropic turbulence being distorted close to the surface of a sphere of radius  $L_0$ .)

Biringen & Reynolds (1981) have used the full nonlinear turbulence equation (with some filtering of the smallest scales) to compute the change in turbulence in the source layer. Their results shown in figure 7(b) are compared with (2.20b) and with Thomas & Hancock's (1977) wind-tunnel measurements. (A further interesting consequence of this argument is that it implies that  $\overline{w^3}, \overline{wu^2}, \overline{wv^2}$  are all *negative* and that the turbulent energy in excess of the value predicted from linear theory is to be expected where  $\kappa_1 \sim z^{-1}$ , as TH observed.)

We can also compare (2.20a) with the computed and measured *rate of growth* of the turbulence in the source layer:  $(1/\bar{u}^2) d\bar{u}^2/dt \approx 0.03U/L_0$ . Since the observed turbulence intensity  $(\bar{u}^2)^{1/2}/U \approx 0.04$ , the agreement with (2.20a) is well within a factor of 2.

(An interesting result of TH's experiments was that the amplification of  $\bar{u}^2$  was much greater than  $\bar{v}^2$ . Although the velocity shear was small ( $L_0(dU/dz)/U \sim 1\%$ ), over a time  $\sim L_0/u_0$  the total strain ( $\sim 4$  and  $\sim 1$  in the two experiments) was sufficient to distort the eddies so as to reduce the scale of  $w$  in the lateral direction (i.e. reduce  $L_y^{(w)}/L_x^{(w)}$ ) (Townsend 1976, p. 110). Then the straining of  $\omega_y$  by impinging eddies became greater than that of  $\omega_x$ , and hence  $\bar{u}^2$  had to be greater than  $\bar{v}^2$ . Although TH varied the speed of the boundary relative to the freestream by 5%,  $dU/dz$  was changed only over a distance  $z < \frac{1}{3}L$ , which therefore does not much affect this argument.)

In a developing convective boundary layer near a surface, one might expect this amplification to be *less* near a lower surface and *greater* near an upper surface because the downdraughts in a convective layer contain less small-scale turbulence than the updraughts (Lenschow & Stephens 1980).

## 2.2. Turbulence near a boundary in steady flow

### 2.2.1. Proposed velocity field

It is *observed* that in laterally homogeneous thermal convection boundary layers (CBLs) and shear-free boundary layers (SFBLs) that the mean rate of energy dissipation per unit mass  $\epsilon$  is approximately constant with height. As a good approximation we assume  $\partial\epsilon/\partial z = 0$ , or, more precisely,

$$\epsilon^{-1} \left| \frac{d\epsilon}{dz} \right| \ll L_0^{-1}. \quad (2.21)$$

For any fully developed turbulent flow, as  $R \rightarrow \infty$ , where  $R = u_0 L_0/\nu$ , the mean square of the sum of the velocity gradients that determine  $\epsilon$  is proportional to the mean square of the vorticity  $\boldsymbol{\omega} = \nabla \times \mathbf{u}$ . Thence (see Townsend 1976, p. 42).

$$\epsilon = \nu \overline{|\boldsymbol{\omega}|^2}, \quad (2.22a)$$

and, from (2.21),

$$\frac{\partial \overline{|\boldsymbol{\omega}|^2}}{\partial z} = 0. \quad (2.22b)$$

Thus the mean-square vorticity (which is determined by microscale eddies ( $\sim R^{-2}L_0$ )) and the eddies in the inertial subrange (where they are small enough not to impact on the surface), are independent of  $z$ .

(We recall for comparison that, in shear flows of thickness  $z_1$ , near the surface where  $z/z_1 \rightarrow 0$ ,  $\epsilon \propto z^{-1}$  and  $\overline{|\boldsymbol{\omega}|^2} \propto z^{-1}$ .)

However, it is observed that all the components of the mean-square turbulent velocity, and the turbulence integral scales vary with height. Our aim is to develop a model for  $\mathbf{u}$  such that the following conditions are satisfied in (2.21).

(i) The turbulence in the central region of a convective layer is an approximately homogeneous turbulent flow  $\mathbf{u}^{(H)}$ , in the sense that a typical integral scale  $L_0$  is small compared with the thickness  $z_1$  of the layer (in fact  $L_0 \approx \frac{1}{4}z_1$ ).

(ii) The vertical component of turbulence tends to zero when  $z$  is small compared with  $L_0$ . (The reason why this boundary condition is not applied in most shear flows is because most of the eddies at height  $z$  are smaller than the distance to the ground. Typically  $L_x^{(w)} \approx (0.5 \pm 0.1)z$ , so the proportion of  $\bar{w}^2$  affected directly by the ground is less than 20%.)

(iii) The flow is incompressible. Thus

$$\mathbf{u} \rightarrow \mathbf{u}^{(H)}(x, t) \quad (z/L_0 \gg 1), \quad (2.23a)$$

$$\mathbf{u} \cdot \mathbf{n} \rightarrow 0 \quad \text{as } z/L_0 \rightarrow 0, \quad (2.23b)$$

and

$$\nabla \cdot \mathbf{u} = 0. \quad (2.24)$$

*Hypothesis:* given (2.21) and then (2.22), the simplest solution to (2.24) subject to (2.23) is that

$$\mathbf{u} = \mathbf{u}^{(H)} + \mathbf{u}^{(s)}, \quad (2.25)$$

where  $\mathbf{u}^{(s)}$  is a source-like irrotational velocity field, which is chosen to satisfy (2.23). Thus

$$\frac{\partial}{\partial z} \overline{(\mathbf{u}^{(H)})^2} = 0, \quad \nabla \times \mathbf{u}^{(H)} = \nabla \times \mathbf{u} = \boldsymbol{\omega}^{(H)}, \quad (2.26a)$$

$$\nabla \times \mathbf{u}^{(s)} = 0, \quad \nabla \cdot \mathbf{u}^{(s)} = 0 \quad (2.26b)$$

and

$$\mathbf{u}^{(s)} \cdot \mathbf{n} = \mathbf{u}^{(H)} \cdot \mathbf{n} \quad \text{as } \frac{z}{L_0} \rightarrow 0, \quad (2.26c)$$

$$\mathbf{u}^{(s)} \rightarrow 0 \quad \left( \frac{z}{L_0} \gg 1 \right). \quad (2.26d)$$

The implication of this hypothesis is that  $\mathbf{u}$  is approximately the same as that obtained in §2.1 for the flow near a suddenly introduced boundary. In §3 we discuss the comparison between velocity measurements in the convective boundary layer and this model. In §2.2.2 we consider where the model is likely to be in error.

### 2.2.2. Some justifications of the model

There are two causes for any systematic differences between the vorticity  $\boldsymbol{\omega}$  near  $z = 0$  and its value  $\boldsymbol{\omega}^{(H)}$  well above a SFBL or its value in the centre of a CBL:

(i) the systematic distortion of the small-scale vorticity by large-scale eddies impinging on the surface (the terms  $-(\mathbf{u} \cdot \nabla) \boldsymbol{\omega} + (\boldsymbol{\omega} \cdot \nabla) \mathbf{u}$  in (2.3)) as discussed in §2.1.2; and

(ii) the variation in the rotational buoyancy force near the surface (the term  $\nabla p \times \nabla(1/\rho)$  in (2.3)), which is equivalent in the Boussinesq approximation to  $-g\hat{\mathbf{z}} \times \nabla\theta/\bar{\theta}_0$ , where  $\hat{\mathbf{z}}$  is the unit vector in the vertical.

*Measurements* of the spectrum of  $\theta$  in a convective boundary layer (e.g. Kaimal *et al.* 1976) show that the large-scale components (i.e.  $\kappa_1 z \ll 1$ ) do not vary significantly with  $z$ . But in eddies of the scale of  $z$  and smaller, the temperature fluctuations increase rapidly near the ground. (These measurements are consistent with the common observations that the temperature fluctuations of the large ‘thermals’ – which are characteristic of the centre of a CBL – are measurable at the surface. But it is also observed that these large thermals consist of an accumulation of many smaller thermals developing from near the ground. See for example Lenschow & Stephens (1980).)

The dynamical consequences of this structure of the temperature field are that, when  $\kappa_1 z \ll 1$ , the rotational buoyancy forces near the surface should not be significantly different from those in the centre of the CBL. Nor should the nonlinear vorticity distortion amplify  $\boldsymbol{\omega}$  at the low wavenumbers.

However, when  $\kappa_1 z \gg 1$ , the larger temperature fluctuations are observed not to change the form or magnitude of the velocity spectra. One possible reason for this is that the *timescale* of the temperature fluctuations ( $O(\epsilon^{-1/3} \kappa_1^{-2/3})$ ) is not large enough

for the buoyancy forces to affect  $\Theta_{33}$ ; this is consistent with the fact that  $\theta$  and  $\omega$  are not well-correlated at high wavenumbers. Wyngaard & Coté (1972) observed that  $\Theta_{3\theta} \propto \kappa_1^{-\frac{1}{2}}$  when  $\kappa_1 z \gg 1$ .

Thus it seems that only when  $\kappa_1 \sim z^{-1}$  can surface buoyancy effects or the vorticity distortion effects change  $\omega$  from its value in the centre of the CBL. The order of magnitude of the change of  $\omega$  due to these effects over a limited wavenumber range is  $O(1)$ . The effects of the surface vorticity distortion on  $\omega$  were estimated in §2.1.2; the effects of surface buoyancy forces on  $\omega$  have not been estimated; but their effects on  $\overline{w^2}$  and on  $\Theta_{33}$  appear to be small, as comparisons between the theory and experiment indicate.

Another way of understanding and estimating the rate of energy transfer  $\epsilon(k)$  is first to consider in homogeneous turbulence the straining  $\int_0^k k^2 E dk$  by eddies larger than  $k^{-1}$  on a timescale characteristic of the large eddies,  $(\int_0^k k^2 E dk)^{-\frac{1}{2}}$ . This straining acts on small-scale eddies with energy  $\int_k^\infty E dk$ . Then (Townsend 1976, p. 99)

$$\epsilon \approx \left[ \int_k^\infty E dk \right] \left[ \int_0^k k^2 E dk \right]^{\frac{1}{2}}.$$

This estimate shows that, if in a boundary layer straining by the large eddies tends to infinity or zero as  $z/L \rightarrow 0$ , then it would be impossible for  $\epsilon$  to be constant. Hence the mean square vorticity of the large eddies is bounded above and below as  $z \rightarrow 0$  (unlike the case of a shear flow). This provides some support for the hypothesis that  $k^2 E(k) \approx \text{constant}$ , and therefore the spectrum of vorticity for all wavenumbers is constant.

In the next section we consider a physical interpretation of this model when we compare it with experimental results.

### 3. A comparison of the theory with turbulence measurement in CBL and SFBLs

#### 3.1. Similarities

##### 3.1.1. Dissipation rate $\epsilon(z)$

The theory of §2 suggested that the turbulence structure near a rigid surface is controlled by the form of the high wavenumber part of the spectrum of turbulence near the surface. If the Reynolds number of the turbulence is large enough (say  $u_0 L_0/\nu \geq 10^3$ ) then the relevant part of the spectrum is the inertial subrange

$$\Theta_{33} = \alpha_K \epsilon^{\frac{1}{3}} \kappa_1^{-\frac{2}{3}}, \quad (3.1)$$

which is determined by  $\epsilon$  and the Kolmogorov constant  $\alpha_K$ . If the Reynolds number (R) is only moderate (say  $u_0 L_0/\nu \sim 10^2$ ) as in the laboratory grid turbulence of TH, then it is observed that the high-wavenumber spectrum has the form of (3.1) provided that the actual dissipation  $\epsilon$  is replaced by  $\epsilon_s$ , a suitable 'spectrum' energy-transfer rate where  $\epsilon > \epsilon_s$ . (Such a procedure may also be necessary in laboratory convection experiments.)

To compare measurements in CBLs and SFBLs with the theory, we express  $\epsilon$  in CBLs in terms of the distance  $z$  above the surface, the boundary-layer thickness  $z_1$ , and the boundary-layer surface buoyancy flux  $gQ/(\theta_0 \rho C_p)$  (written as  $w_*^3/z_1$ ). To compare measurements in CBLs and SFBLs with each other and with the theory we also express  $\epsilon$  (and  $\epsilon_s$ ) in terms of the r.m.s. vertical turbulent velocity  $w_0$  and the integral lengthscale  $L_0 = L_x^{(w)}$ , of the vertical component in the middle of the convective layer (CBL) ( $z \sim 0.5z_1$ ) or outside the SFBL.

*CBL.* In strongly convective conditions (i.e.  $w_*/u_* \geq 5$ ) where  $u_* = (\tau_s/\rho)^{\frac{1}{2}}$ ,  $\tau_s$  being

the surface shear stress,  $\epsilon(z)$  is observed to vary by less than 15% over the range  $0.1 < z/z_1 < 0.9$ . The magnitude of  $\epsilon$  is found to be (e.g. Caughey & Palmer 1979)

$$\epsilon \approx (0.55 \pm 0.1) \frac{w_*^3}{z_1}.$$

Since  $w_0^2 \approx 0.4w_*^2$  and  $L_x^{(w,0)} \approx \frac{1}{4}z_1$

$$\epsilon \approx (0.55 \pm 0.1) \frac{w_0^3}{L_x^{(w,0)}}, \quad (3.1)$$

where subscript or suffix 0 indicates the value in the centre of the CBL. Here  $\epsilon$  is measured directly from the very small-scale velocity gradients using Taylor's formula (Batchelor 1953)

$$\epsilon = 15\nu \overline{\left(\frac{du}{dx}\right)^2}. \quad (3.2)$$

*SFBL.* Measurements of grid turbulence in a wind tunnel by TH near a wall moving at the same speed as the mean flow showed that  $\epsilon(z)$ , in this case the rate of decay of the turbulent energy, was approximately constant with  $z$  (at least to within 15%), with magnitude

$$\epsilon \approx 1.5 \frac{w_0^3}{L_x^{(w,0)}}. \quad (3.3)$$

In the high-wavenumber part of their spectrum they observed that  $\Theta_{11}$  was described by the von Kármán spectrum, so that

$$\Theta_{11}(\kappa_1) \approx 0.2w_0^2(L_x^{(w,0)})^{-\frac{2}{3}}\kappa_1^{-\frac{5}{3}}. \quad (3.4)$$

Thence taking  $\alpha_K = 0.25$ , (3.4) can be expressed in terms of  $\epsilon_s$ , where

$$\epsilon_s = (0.72 \pm 0.05) \frac{w_0^3}{L_x^{(w,0)}}. \quad (3.5)$$

### 3.1.2. Vertical turbulence

*CBL.* Atmospheric measurements (e.g. Panofsky *et al.* 1977; Caughey & Palmer 1979), where  $R \sim 10^7$ , show that when  $z/z_1 \rightarrow 0$  (but  $z/z_1 \gg (u_*/w_*)^{\frac{3}{2}}$ )

$$\overline{w^2} \approx 1.8 \left(\frac{w_*^3}{z_1}\right)^{\frac{2}{3}} z^{\frac{2}{3}} \quad (3.6a)$$

or

$$\overline{w^2} \approx (2.4 \pm 0.4) \epsilon^{\frac{2}{3}} z^{\frac{2}{3}}. \quad (3.6b)$$

Note that laboratory measurements of  $\overline{w^2}$  by Adrian & Ferreira (1979), where  $R \sim 10^3$ , agree with the limiting form of (3.6a) but increase in a shorter distance to their value in the centre of the CBL than the atmospheric data (see figure 4). (Note that in a shear boundary layer where  $\epsilon$  varies as  $\epsilon \approx u_*^3/0.4z$ , and  $(\overline{w^2})^{\frac{1}{2}} \approx 1.3u_*$ ,  $\overline{w^2}(z)$  can be expressed in the form of (3.6b) as  $\overline{w^2} = 0.9[\epsilon(z)]^{\frac{2}{3}} z^{\frac{2}{3}}$ , but with a considerably smaller constant.)

*SFBL.* Wind-tunnel measurements by TH for a developing SFBL show that when  $z \ll L_x^{(w,0)}$

$$\frac{\overline{w^2}}{w_0^2} \approx 1.4 \left(\frac{z}{L_x^{(w,0)}}\right)^{\frac{2}{3}},$$

or, in terms of the spectral dissipation  $\epsilon_s$ ,

$$\overline{w^2} \approx 1.8\epsilon_s^{\frac{2}{3}} z^{\frac{2}{3}}. \quad (3.7)$$

Measurements of rather low-Reynolds-number turbulence produced by an oscillating grid near a rigid surface also decrease in a distance of the order of  $L_0$  (McDougall 1979).

The data for CBL and SFBLs are plotted in figure 4 together with the theory. In the limit  $z/L_x^{(w,0)} \ll 1$ , if  $\alpha_K = 0.25$ , the theory (given by (2.14*b*)) is close to the results for the SFBL, but less by one-fourth than those of the CBL. For comparison with the theory, the turbulence in the centre of the CBL is assumed to be approximately homogeneous, so that  $\overline{w^2}/w_0^2$  is compared with  $\overline{w^2}/w^{2(H)}$ .

### 3.1.3. Horizontal turbulence

*CBL.* In the centre of a CBL  $(\overline{u_0^2})^{1/2}/w_0 \approx 0.9$ , while near the ground the inversion layer  $(\overline{u^2})^{1/2}$  increases. Typically (Caughey & Palmer 1979; Deardorff & Willis 1974; Adrian & Ferreira 1979) when  $z/L_x^{(w,0)} \approx 0.2$

$$\overline{u^2} \approx (1.5 \pm 0.3) \overline{u_0^2}. \quad (3.8)$$

Within a distance  $l_v$  from a smooth surface of about  $2(L_x^{(w,0)} \nu)^{1/2}/w_0$  viscous effects reduce  $\overline{u^2}$  according to the predictions of HG (see p. 234) and observations in Adrian & Ferreira's (1979) laboratory experiment where  $L_x^{(w)} w_0/\nu \sim 200$ ,  $l_v/z_i \sim 0.05$ , which is close to the estimate of about 0.04.

*SFBL.* With grid turbulence in a wind tunnel, TH found that outside the SFBL  $(\overline{u_0^2})^{1/2}/w_0 \approx 1.1$ , while near the surface

$$\frac{\overline{u^2}}{\overline{u_0^2}} \approx 1.8 \quad \text{at} \quad \frac{z}{L_0^{(w)}} \approx 0.1. \quad (3.9)$$

In McDougall's (1979) experiment with an oscillating grid  $w_0 L_0/\nu \sim 40$ , and  $l_v/L_x$  was observed to be about  $\frac{1}{5}$ ; the estimate gives  $\frac{1}{3}$ .

### 3.1.4. Spectra and integral scales

*CBL.* The wavelength  $\lambda_m^{(w)}$  at which  $\kappa_1 \Theta_{33}(\kappa_1)$  is a maximum is more easily obtained from the spectra than the integral scale of the vertical turbulence  $L_x^{(w)}$ . However, for any of the empirical forms of spectra used by Kaimal *et al.* (1976) or Kaimal (1978) or HG, it is found that  $\lambda_m \approx 6L_x$ .

The integral scale has its maximum value in the middle of the CBL at  $z/z_i = 0.5$ , where

$$\lambda_m^{(w)} \simeq 1.5z_i, \quad L_x^{(w,0)} \approx 0.25z_i. \quad (3.10a)$$

This means that for most of the energy-containing scales the turbulence near the surface is effectively uncorrelated with (though not independent of) the turbulence near the upper boundary layer of the convective layer at  $z = z_i$ .

Then, using Caughey & Palmer's (1979) summary of the observations of  $L_x^{(w)}/z_i$ , the ratio  $L_x^{(w)}(z)/L_x^{(w,0)}$  is plotted against  $z/L_x^{(w,0)}$  in figure 5. Caughey & Palmer noted that, asymptotically when  $z/z_i \ll 1$ , the integral scale has the form

$$\lambda_m^{(w)} \approx 6.0z \quad \text{or} \quad L_x^{(w)} \approx 1.0z. \quad (3.10b)$$

Figure 5 shows that these observations agree to within 20% with the calculation of HG for  $z/L_x^{(w,H)} < 1$  or  $z/z_i < 0.25$ . In fact, the experimental asymptote agrees with the *theoretical* computation to this accuracy for  $0.2 < z/L_x^{(w,H)} < 0.06$ . The computations only agree to within 20% with the *theoretical* asymptote when  $z/L_x^{(w,H)} < 0.01$ . Therefore (3.10*b*) can be regarded as the appropriate limit for practical purposes.

Kaimal (1978) has found that  $\Theta_{11}(\kappa_1 \rightarrow 0)$  is independent of height and is given

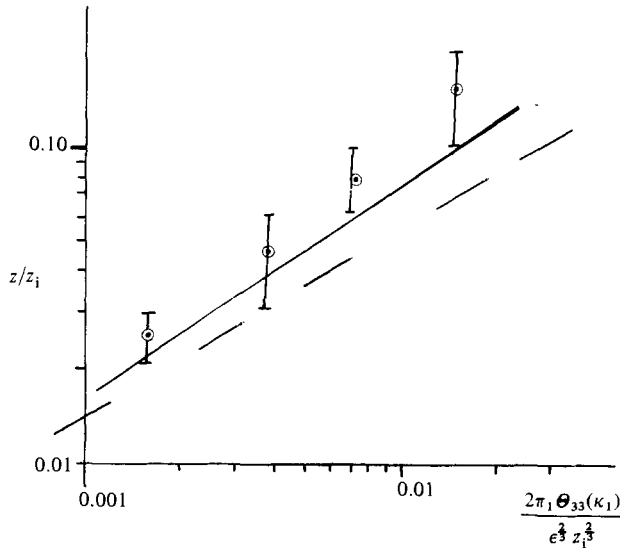


FIGURE 8. Variation of low-frequency spectrum of vertical velocity with height. Atmospheric measurements of Kaimal *et al.* (1976) at  $\kappa_1 = 0.6z_1^{-1}$ : —, theory ((2.12) as  $\kappa_1 \rightarrow 0$ ); ---, asymptotic limit ( $z/z_1 \rightarrow 0$ , (2.13)).

approximately by  $\overline{u^2}z_1/4\pi$  (i.e. in his notation  $S(n \rightarrow 0) = \frac{1}{4}\overline{u^2}z_1$ ). (Note that  $\overline{u^2}$  increases when  $z/z_1 \rightarrow 0$  in some observations, but this is not observed to change  $\Theta_{11}(\kappa_1 \rightarrow 0)$ .)

At high wavenumbers, the spectra have the same form for all  $z$ , i.e. when  $\kappa_1 \lesssim 1/z_1$

$$\Theta_{11}(\kappa_1) \approx \alpha_K \epsilon^{3/2} \kappa_1^{-5/2}. \tag{3.11}$$

The measurements of the spectrum  $\Theta_{33}(\kappa_1)$  by Kaimal (1978) (though not described in quite this way) show that when  $\kappa_1 \gg z^{-1}$  the spectrum has the Kolmogorov inertial-subrange form

$$\Theta_{33}(\kappa_1) = \frac{4}{3}\alpha_K \epsilon^{3/2} \kappa_1^{-5/2}$$

where  $\alpha_K \approx 0.25$ .

To test the theory at low frequency (where atmospheric measurements are especially difficult), the predictions (2.12) and (2.13) are compared in figure 8 with measurements, at a particular frequency ( $\kappa_1 = (2\pi/10)z_1^{-1}$ ), of the variation of the spectrum of  $w$ . The normalized spectrum  $2\kappa_1 \Theta_{33}(\kappa_1) / (\epsilon^{3/2} z_1^{3/2})$  is plotted as a function of  $z/z_1$ , when  $z/z_1 \ll 1$  and  $\kappa_1 \ll z^{-1}$ . The data are taken from figure 3 of Kaimal *et al.* (1976). It appears that, at the lowest values of  $z/z_1$ , the 20% systematic difference between observations and theory is of the same order as experimental error. Note that as  $z/z_1 \rightarrow 0$  the asymptotic form for  $\Theta_{33}$ , viz

$$\Theta_{33}(\kappa_1 \rightarrow 0) \propto \epsilon^{3/2} z_1^{3/2} \tag{3.12}$$

is only *theoretically* accurate to 15% when  $z/z_1 < 0.01$ .

In figure 6(c) measurements of cross-correlations of the vertical velocity at different heights (provided  $z < z_1 \ll z_i$ ) (on different days and with different relative intensities of thermal-to-shear turbulence, as measured by  $w_*/u_*$ ) are compared with the theoretical results, described in §2. The predictions that  $\overline{w(z_1)w(z)} \propto z$  as  $z \rightarrow 0$  and  $\overline{w(z_1)w(z)}/\overline{w^2(z_1)}$  is a function of  $z/z_1$  are borne out rather convincingly. This asymptotic prediction is not as dependent as (3.12) on the smallest scales of turbulence, and so appears to be valid even when  $z < 0.1z_1$  and  $z_1 < 0.1z_i$ .

*SFBL.* The wind-tunnel measurements show that when  $z/L_0 \ll 1$

$$L_x^{(w)} \approx 1.0z, \tag{3.13a}$$

and when  $z \simeq 2L_x^{(w,0)}$

$$L_x^{(w)} \approx 0.8L_x^{(w,0)}, \quad (3.13b)$$

whereas  $\overline{w^2}/\overline{w^{2(H)}} \approx 1.0$ . This shows how the large scales are affected by the wall to a greater distance than  $w^2$ .

The measured values of  $L_x^{(w)}$  in the CBL and in TH's experiment for the SFBL are plotted in figure 5 along with the theory. It is difficult to tell whether the theoretical limit (2.15) agrees with the observations. For practical purposes, when  $z/L_0 < 0.1$ , the observations as described by (3.10a) and (3.13a) agree well with the theoretical computations for the typical form of  $E(k)$  given in (2.13c).

### 3.2. Discussion of the differences and similarities

In the discussion of turbulence in a developing SFBL without buoyancy forces, it was suggested in §2.1.3 that the straining of small-scale turbulence by large-scale eddies impinging on the wall leads to *negative* values of  $\overline{w^3}$  and  $\overline{u^2w}$ . However, in a CBL it is observed that both these third-order moments are *positive*; by similarity arguments or inspection of the equation governing the growth of third-order moments, it is expected that when  $z \ll z_1$

$$\overline{w^3} \propto \epsilon z. \quad (3.14a)$$

The buoyancy term in the third-order moment equation,  $g\overline{w^2\theta}/\theta_0$ , is the main cause for the positive skewness (Wyngaard 1979). Laboratory data, and atmospheric data obtained from information on aircraft and towers, show that for  $z < 0.2z_1$

$$\overline{w^3} \approx (1.0 \pm 0.25) \epsilon z \quad (3.14b)$$

(Hunt *et al.* 1984; Lenschow, Wyngaard & Pennell 1980).

The physical reason for this skewness is that buoyancy forces affect the structure of turbulence at a scale of order  $z$ , as well as the largest scale  $z_1$ . In other words, it is only a useful approximation for second-order moments to regard the turbulence structure near the ground as largely the distortion of small-scale isotropic turbulence caused by the boundary condition of zero vertical velocity at the ground.

At first sight this physical model has little relation to the description of convective turbulence, developed by Priestley (1959), as largely an assembly of converging thermal plumes which are narrow near the ground and entrain each other into larger plumes as they rise. Between the plumes, cooler air sinks with relatively smaller velocities. With arrays of ground-level instruments (Wilczak & Tillman 1980) and analysis of aircraft-mounted probes (Lenschow & Stephens 1980), this physical picture has been substantiated and quantified; for example, in the variation with height of the shape, the diameter and the number of thermal plumes per unit area.

However, there should be no contradiction between that model and the one presented here if we recognize that this is a statistical model. For example, this model suggests that small-scale turbulence is the largest contribution to the vertical variance near the ground. This turbulence is probably mainly produced by the intense almost-isotropic turbulence in the shear layers bounding the rising thermals. However, the scales of these eddies, which are of the order of their height  $z$  above the ground, are large enough that they are confined by the boundary at  $z = 0$ . In other words, one can think of the rising thermals as having *image* thermals below the ground to ensure that  $w = 0$  at  $z = 0$ , as suggested in figure 9.

This picture conveys the essence of the model presented here, though it is perhaps surprising what a strong effect these 'image' thermals have and how by considering their effect, so much can be deduced just in terms of the mean rate of energy dissipation.

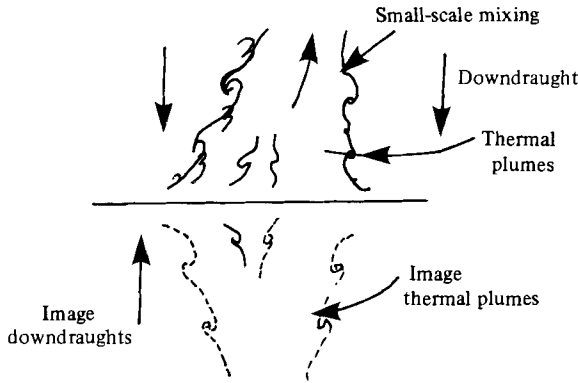


FIGURE 9. Schematic diagram of 'image' thermal plumes; an essential qualitative feature so that  $w = 0$  at  $z = 0$ .

#### 4. Effects of mean-velocity gradients near the surface

We have assumed so far that, if a mean velocity  $U$  exists it is uniform, so that at  $z = 0$  the bottom surface moves or else there is an infinitesimally thin boundary layer. We now consider briefly the turbulence near  $z = 0$  when there is an inner shear layer of thickness  $\delta \ll L_0$ , where  $L_0 = L_x^{(w, 0)}$ . Let the surface shear stress be  $\rho u_*^2$  (figure 10).

When  $z > \delta$  the turbulence of the inner layer decays and one expects that its effect on the external turbulence is negligible. But, whatever the value of  $u_*/w_0$  at some value of  $z < \delta$ , the vertical components of the shear-driven turbulence ( $w_s$ ) and the external turbulence ( $w_e$ ) are of the same order of magnitude, since  $w_e \rightarrow 0$  as  $z \rightarrow 0$ . If  $\delta \ll L_x^{(w, 0)}$ , the interaction of  $w_e$  with the velocity gradient  $dU/dz$  is weak, according to the rapid-distortion calculations of Durbin (1979), and any direct interaction between  $u_e$  and  $u_s$  by the vortex-stretching mechanisms of §2.1.2 is weaker by  $O(\delta/L_0)$  than the self-induced effects of  $u_e$  on itself. These are plausible physical reasons to expect that  $u_s$  and  $u_e$  are statistically independent when  $\delta \ll L_0$ . In that case

$$\overline{u^2} \approx a_1^2 u_*^2 f_u \left( \frac{z}{\delta} \right) + \overline{u_e^2} \left( \frac{z}{L_0} \right), \quad (4.1)$$

$$\overline{w^2} \approx a_3^2 u_*^2 f_w \left( \frac{z}{\delta} \right) + \overline{w_e^2} \left( \frac{z}{L_0} \right), \quad (4.2)$$

where  $a_1$  and  $a_3$  are the measured turbulence structure parameters, which Townsend's (1976, p. 107) table give as  $4 < a_1 < 6.25$  and  $a_3 \approx 1.7$ . The functions  $f_u, f_w$  are taken as the measured variations of  $\overline{u^2}, \overline{w^2}$  in the shear layer in the absence of external turbulence. Typically

$$\left. \begin{aligned} f_u \approx f_w \approx 1.0 \quad \left( \frac{z}{\delta} < 0.2 \right), \\ f_u, f_w \left( \frac{z}{\delta} \right) < 0.1 \quad \left( \frac{z}{\delta} \gtrsim 1 \right) \end{aligned} \right\} \quad (4.3)$$

If  $\delta/L_0 < 0.05$ , from §§2.1 and 3.1,  $\overline{u_e^2} \approx (1.5 \pm 0.5) \overline{u_0^2}$ ,  $\overline{w_e^2} \approx 7\alpha_K(\epsilon_e)^{\frac{1}{2}} z^{\frac{3}{2}}$ , where  $\epsilon_e$  is the dissipation in the external turbulence. For values of  $\delta/L_0$  greater than, say,  $\frac{1}{4}$ , the external turbulence can amplify and diffuse upward some of the shear-generated turbulence and some of the surface Reynolds stress. In that case  $f_u, f_w(z)$  could be greater and extend further upwards than in the absence of external turbulence.

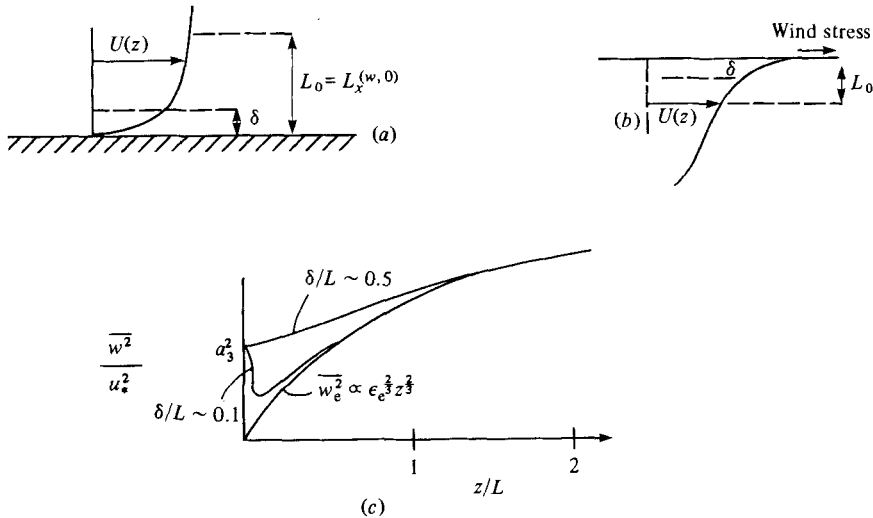


FIGURE 10. Large-scale turbulence near surfaces where there is a thin shear layer: (a) on a rigid surface; (b) at a free surface; (c) typical profiles of  $\overline{w^2}$  for different values of  $\delta/L$ .

Wind-tunnel measurements have been made of the interaction of large-scale external turbulence and developing thin boundary layers. (a) Over an aerofoil boundary layer, where  $\delta/L_0 \approx 0.2$ , it was found that  $\overline{w^2}$  decreased near the surface outside the shear layer, where  $z > \delta$ , before increasing inside the boundary layer  $z < \delta$  (Graham 1975; the data are plotted on figure 5 of HG). (b) Near a boundary layer on a wind-tunnel wall where  $\delta/L_0 \approx 0.8$  and  $u_* \sim (\overline{u_e^2})^{1/2}$  it was found that  $\overline{w^2}$  monotonically decreased as  $z \rightarrow 0$  (Petty, unpublished). These two kinds of behaviour are consistent with (4.1) and (4.3). (c) In zero-pressure-gradient boundary layers on a flat plate where  $\delta \sim L_0$  and  $u_* \sim (\overline{w_e^2})^{1/2}$  the maximum values of  $f_u$  and  $f_w$  were found by Arnal, Cousteix & Michel (1976) to be largely unaffected by external turbulence, but there was indeed some upward diffusion of the boundary-layer turbulence by a distance of order  $\delta$ .

In the CBL the thickness of the shear layer on  $z = 0$  is not determined by external constraints as in the two developing wind-tunnel flows. It is observed that when  $0 \leq u_*/w_* \leq 0.25$  or  $u_*/w_0 < 0.25$ , the shear-layer thickness is (0.4 to 0.8)  $L_0$ , and that

$$\begin{aligned} \overline{u^2} &\approx a_1 u_*^2 + \overline{u_e^2}, \\ \overline{w^2} &\approx a_3 u_*^2 + \overline{w_e^2}(z) \\ &= 1.7u_*^2 + 7\alpha_K \epsilon_e^{2/3} z^{5/3}. \end{aligned} \quad (4.4)$$

Thus  $(\overline{w^2})^{1/2} > (\overline{w_e^2})^{1/2}$  when  $z/z_1 < (u_*/w_*)^{3/5}$ . So effectively in the CBL

$$\delta \sim z_1 \left( \frac{u_*}{w_*} \right)^{3/5} \quad \text{or} \quad \frac{\delta}{L_0} \sim \frac{1}{4} \left( \frac{u_*}{w_*} \right)^{3/5}. \quad (4.5)$$

Equations (4.4) are the results obtained by Panofsky *et al.* (1977), and were explained in terms of the convective 'mixed-layer' turbulence affecting the surface shear layer, rather than in terms of the statistical independence of the two kinds of turbulence.

If the assumption of statistical independence applies to the variances, it should also apply to the spectra; the empirical expressions developed by Kaimal (1978) to

describe the measurements do indeed satisfy this criterion *even* at the highest wavenumbers.

For example, when  $\kappa_1 \gg \delta^{-1}$  (or  $L_0^{-1}$ )

$$\Theta_{33}(\kappa_1) = \frac{4}{3}\alpha_K [\epsilon_s^{\frac{2}{3}}(z) + \epsilon_e^{\frac{2}{3}}] \kappa_1^{-\frac{5}{3}}, \quad (4.4)$$

where energy dissipation in the shear layer  $\epsilon_s = u_*^3/(0.4z)$ . For the horizontal components at low wavenumber, it is interesting to note that

$$\Theta_{11}(\kappa_1 \rightarrow 0) = \left( u_s^2 L_x^{(u,s)}(z/\delta) + u_e^2 L_x^{(u,0)} \right) \pi^{-1}, \quad (4.5)$$

where  $L_x^{(u,s)}$  is of the order of the shear-layer thickness  $\delta$  and is the integral scale of the  $u$ -component of turbulence produced in the shear layer. Therefore the external turbulence dominates the low-frequency horizontal turbulence, even well within the inner shear layer.

The same arguments used here may well have a wider validity wherever large-scale intense freestream turbulence exists outside an inner boundary layer. (Some comments to this effect were also made by Bradshaw 1978.)

## 5. Discussion

### 5.1. Previous analyses

Previous analyses of turbulence in the CBL (Priestly 1959; Wyngaard, Coté & Izumi 1971) have been largely based on the dimensional argument that the turbulence structure is determined by the buoyancy flux  $g\overline{w\theta}/\theta_0$  at the ground, the height above the ground, and the inversion height  $z_1$ . Some physical justification for these dimensional forms came from the observation that the vertical motion in a CBL resembles buoyant plumes rising from the surface. This approach led to a number of significant predictions, e.g.  $w^2 \propto z^{\frac{1}{3}}$ . But, inevitably, it could not provide much insight into spectral forms or the connection with the nonconvective SFBL. Having said that, the kinematic theory presented here does not contradict these models; its aim is to demonstrate some common aspects of the kinematical structure of all shear-free boundary layers.

In the analysis presented here, the primary assumption is that in shear-free flows, where  $\partial\epsilon/\partial z \approx 0$  over a scale  $L_0$ , there is a simple turbulence structure which satisfied this constraint and the boundary condition on  $z = 0$ . This, *formally*, is a different problem to the initial *development* of a flow of homogeneous weak turbulence as it impinges onto a flat plate. In that case, no assumption is needed about  $\epsilon(z)$  or about the form of the turbulence; both followed from the boundary conditions. However, the solution is the same as that proposed here for SFBLs and CBLs.

### 5.2. Validity of the analysis

The comparison between the kinematic theory and the measurements of variance, integral scale, cross-correlation and spectra indicates that the theory provides a physical reason why the turbulence of CBLs and SFBLs should have an approximately similar structure, near the wall, why the vertical turbulence near the boundary should be determined by  $\epsilon$  and  $z$  only, and why their turbulence structure may differ when  $z \sim L_0$  because of different forms of their spectra far from the surface.

The arguments of §§2.2 show why in SFBLs the linear model cannot allow for some important nonlinear amplification of  $u, v$ ; in §3.2 we showed how it cannot describe how buoyancy forces affect some aspects of the turbulence even very close to the

surface. The simple model is therefore also useful as an indicator of the *differences* between SFBLs and CBLs.

The usefulness of the model has been demonstrated by its prediction of two-point cross-correlations, which, on being measured, agree well with the theory. Further uses of the model have been mentioned in §1.

This paper largely arose from discussion with Dr J. C. Wyngaard and Dr J. C. Kaimal, to whom I am very grateful. I am also grateful to the referees and Dr D. Lenschow (of NCAR) and Mr H. Wong (of DAMTP) for helpful suggestions, and to CIRES, NOAA and NCAR in Boulder, Colorado, for their financial support during visits in 1980, 1982 and 1983.

#### REFERENCES

- ADRIAN, R. J. & FERREIRA, R. T. S. 1979 In *Turbulent Shear Flows 2* (ed. L. J. S. Bradbury *et al.*). Springer.
- ARNAL, D., COUSTEIX, J. & MICHEL, R. 1976 *Recherche Aéronautique* no. 1. 13–16.
- BATCHELOR, G. K. 1953 *The Theory of Homogeneous Turbulence*. Cambridge University Press.
- BIRINGEN, S. & REYNOLDS, W. C. 1981 *J. Fluid Mech.* **103**, 53.
- BRADSHAW, P. 1978 *J. Atmos. Sci.* **35**, 1768.
- CARRUTHERS, D. J. & HUNT, J. C. R. 1983 Velocity fluctuations near an interface between turbulence convection and a stable layer. (Submitted for publication.)
- CAUGHEY, S. J. & PALMER, S. G. 1979 *Q. J. R. Met. Soc.* **105**, 811.
- DEARDORFF, J. W. & WILLIS, G. E. 1974 *Adv. Geophys.* **18B**, 197.
- DURBIN, P. A. 1979 Rapid distortion theory of turbulent flows. Ph.D. dissertation, University of Cambridge.
- DURBIN, P. A. 1981 *Q. J. Mech. Appl. Maths* **34**, 489.
- GRAHAM, J. M. R. 1975 *Imperial Coll. Aero. Tech. Note* 75–101.
- HUNT, J. C. R. 1983 In *Proc. Symp. 'Gas Transfer at Water Surfaces'*, (ed. W. Brutsaert & G. H. Jirka). Reidel.
- HUNT, J. C. R. & GRAHAM, J. M. R. 1978 *J. Fluid Mech.* **84**, 209.
- HUNT, J. C. R., KAIMAL, J. C. & GAYNOR, J. 1984 Measurements of convective turbulence at Boulder Atmospheric Observatory. (Report in preparation.)
- KAIMAL, J. C. 1978 *J. Atmos. Sci.* **35**, 18.
- KAIMAL, J. C., WYNGAARD, J. C., HAUGEN, D. N., COTÉ, O. R., IZUMI, Y., CAUGHEY, S. J. & READINGS, J. C. 1976 *J. Atmos. Sci.* **33**, 2152.
- KOMORI, S., UEDA, H., OGINO, F. & MIZUSHINA, T. 1982 *Intl J. Heat Mass Transfer* **25**, 513–521.
- LENSCHOW, D. H. & STEPHENS, P. L. 1980 *Boundary Layer Met.* **19**, 509.
- LENSCHOW, D. H., WYNGAARD, J. C. & PENNEL, W. T. 1980 *J. Atmos. Sci.* **37**, 1313.
- MCDUGALL, T. J. 1979 *J. Fluid Mech.* **94**, 409.
- PANOFSKY, H. A., TENNEKES, H., LENSCHOW, D. H. & WYNGAARD, J. C. 1977 *Boundary Layer Meteor.* **11**, 335.
- PRIESTLEY, C. H. B. 1959 *Turbulent Transport in the Lower Atmosphere*. University of Chicago Press.
- RODI, W. 1980 *Turbulence Models and Their Applications in Hydraulics*. I.A.H.R. Delft.
- THOMAS, N. H. & HANCOCK, P. E. 1977 *J. Fluid Mech.* **82**, 481.
- TOWNSEND, A. A. 1976 *Structure of Turbulent Shear Flow*, 2nd edn. Cambridge University Press.
- UZKAN, T. & REYNOLDS, W. C. 1967 *J. Fluid Mech.* **28**, 803.
- WILCZAK, J. M. & TILLMAN, J. E. 1980 *J. Atmos. Sci.* **37**, 2424.
- WYNGAARD, J. C. 1979 In *Turbulent Shear Flows 2* (ed. L. J. S. Bradbury *et al.*). Springer.
- WYNGAARD, J. C. & COTÉ, O. R. 1972 *Q. J. R. Meteor. Soc.* **98**, 590.
- WYNGAARD, J. C., COTÉ, O. R. & IZUMI, Y. 1971 *J. Atmos. Sci.* **28**, 1171.